IET Nanobiotechnology

Research Article

IET Journals
The Institution of Engineering and Technology

Engineering molecular communications integrated with carbon nanotubes in neural sensor nanonetworks

ISSN 1751-8741
Received on 9th February 2017
Revised 19th September 2017
Accepted on 11th October 2017
E-First on 22nd January 2018
doi: 10.1049/iet-nbt.2016.0150
www.ietdl.org

Saied M. Abd El-atty[1] ✉, Konstantinos A. Lizos[2], Z.M. Gharsseldien[3,4], Amr Tolba[5,6], Zafer A.L. Makhadmeh[5]

[1]*Department of Electronics and Electrical Communications Engineering, Faculty of Electronic Engineering, Menoufia University, 32952 Menouf, Egypt*
[2]*Faculty of Mathematics and Natural Sciences, University of Oslo (UiO), 0373 Oslo, Norway*
[3]*Department of Mathematics, Prince Sattam Bin Abdulaziz University, 11991 Wadi Adwassir, Saudi Arabia*
[4]*Department of Mathematics, Faculty of Science, Al-Azhar University, Nasr City, 11884 Cairo, Egypt*
[5]*Department of Computer Science, Community College, King Saud University, Riyadh 11437, Saudi Arabia*
[6]*Department of Mathematics, Faculty of Science, Menoufia University, Shebin-El-kom 32511, Egypt*
✉ *E-mail: sabdelatty@el-eng.menofia.edu.eg*

Abstract: There have been recent advances in the engineering of molecular communication (MC)-based networks for nanomedical applications. However, the integration of MC with biomaterials such as carbon nanotubes (CNTs) presents various critical research challenges. In this study, the authors envisaged integrating MC-based nanonetwork with CNTs to optimise nanonetwork performance. In neural networks, a chronic reduction in the concentration of the neurotransmitter acetylcholine (ACh) eventually leads to the development of neurodegenerative diseases; therefore, they used CNTs as a molecular switch to optimise ACh conductivity supported by artificial MC. Furthermore, MC enables communication between transmitter neurons and receiver neurons for fine-tuning the ACh release rate according to the feedback concentration of ACh. Subsequently, they proposed a min/max feedback scheme to fine-tune the expected throughput and ACh transmission efficiency. For demonstration purposes, they deduced analytical forms for the proposed schemes in terms of throughput, incurred traffic rates, and average packet delay.

1 Introduction

Alongside the rapid spread of molecular communication (MC)-based nanonetworks, considered by many to be in its infancy, there have been recent advances in the development of nanotechnology-based biomaterials such as carbon nanotubes (CNTs) for use in neuroscience. There has been particular emphasis on nanobiomedical applications and targeted drug delivery systems (DDSs), with the aim of utilising MC and CNTs for therapeutic purposes and solving cognitive problems in the intra-body nervous nanonetwork [1]. However, their utilisation may face design challenges and serious risks for in vivo applications. In this study, we investigated the assimilation of MC into CNTs to enhance nanonetwork communication performance. We illustrated the development of bio-nanotechnology and engineered neural biomaterials, particularly CNTs, and the possibility of integrating them into biological systems to create an MC system. Further, we attempted to theoretically construct an integrated artificial MC nanonetwork.

MC is currently viewed as a promising approach to transmitting information in the intra-body nanonetwork. A nanomachine is an element of the nanonetwork that facilitates designated operations, e.g. processing, actuation, logic, and sensing [2]. Furthermore, nanomachines have the ability to exchange information when they are interconnected by means of MC [3]. A simple intra-body nanonetwork can be achieved by connecting a group of artificial/synthetic or biological nanomachines to perform complex tasks and functions in the human body, such as biomedical diagnosis and treatment, or neural signal transduction and neural control [4]. We recently investigated the molecular effects of such a system on the electronic structure of a nanomachine in the context of MC-based nanonetwork performance [5]. Recent surveys have illustrated state-of-the-art advances in the area of MC-based nanonetworks [6–8].

The use of nanotechnology in modern neuroscience has enabled therapeutic regenerative strategies by exploiting direct or specific interactions between biological cells and synthetic nanomaterials. In this paper, the nanoscale characteristics and dimensions of CNTs facilitate the molecular interplay among live cells, including neurons [9, 10]. Consequently, experimental studies on MC-based CNT conductors have been carried out [11], and a stable switch-based molecular interconnection for coupling molecules and CNTs has been proposed [12]. Moreover, CNTs offer a novel alternative to therapeutic molecules with regard to MC in the human intra-body nanonetwork [13, 14]. Recently, Malak and Akan [15] of the Next-Generation and Wireless Communications Laboratory have made advances in Information Communication Technology (ICT)-inspired treatment methods for neuronal disease by employing CNTs with the ability to recognise the release of neurotransmitter molecules in the intra-body nervous nanonetwork. Moreover, Akan *et al.* [16] explored the possibility of applying ICT in an intra-body molecular nanonetwork for the treatment and diagnosis of malignant diseases. They concluded that adopting an ICT-based approach benefits the development of smart DDSs for the treatment of Alzheimer's disease, Parkinson's disease, and various heart diseases.

2 Related work and contributions

Typically, in nervous systems, neurons emit electrical spikes, known as action potentials (APs) that are responsible for the release of acetylcholine (ACh) neurotransmitter molecules that propagate down the axon. External stimulation triggers communication between the brain and various parts of the nervous nanonetwork. In such a nanonetwork, the brain enables changes in neuronal excitability, prompts synaptic plasticity and synaptic transmission, and manages the AP of neurons according to the variation in ACh neurotransmitters [17]. ACh facilitates the

reaction or feedback of neural networks in various brain sections, making cholinergic modulation a crucial mechanism underlying complex behaviours. Recent investigations using Raman spectroscopy have confirmed the adsorption of ACh molecules on CNTs [14]. This system effectively delivers ACh to the neurons via the neurite axoplasm and ameliorates the effects of Alzheimer's disease [18], and it is considered the first step towards nanocarriers for drug delivery to the central nervous system (CNS). Subsequently, CNTs have been used as a delivery system for the treatment of CNS pathologies based on their structural features, and the chemical modification of CNTs has also been described [19]. The blood–brain barrier presents a challenge for drug delivery to the brain. However, recent studies have reported the successful deployment of functionalised CNTs for delivering drugs or genes to the brain [20–22]. Evidence supporting the use of CNTs in neuron regeneration has been reported in [23, 24].

Interestingly, a CNT-based multi-electrode array (MEA) biochip has been developed [25] for measuring the concentrations of neurotransmitters, such as dopamine, and electrophysiological responses, such APs. This biochip facilitates real-time investigation of presynaptic and postsynaptic activities and therefore plays a significant role in information processing in the neural network. In the same context, CNTs have been shown to boost the efficacy of signal transmission between the brain and the nervous system [26]. However, recent reports [27–29] have shown that under certain circumstances, the AP may back-propagate to the dendrites. This neural back-propagation phenomenon can influence the ACh release rate and cause fluctuating ACh transmission. This affects the diffusion of ACh over the postsynaptic neuron and consequently, the transmission probability. In this study, we express this fluctuation in ACh transmission as the number of ACh molecules processed by the postsynaptic receptors per unit time, i.e. throughput. Cello *et al.* [27] have proposed the 'electronic hypothesis' to explain the interactions between CNTs and neurons. These authors developed a mechanism to study the effect of CNTs on the efficacy of neural signal transmission in cultured neural networks and discovered that the back-propagation of the AP can be improved by interaction with the CNTs. Moreover, some authors [30, 31] have proposed an artificial neuronal network based on MC system wherein they designed transmission-scheduling protocols and an interface between the bio-nanomachine and the neurons to facilitate signalling initiation and reduce the possibility of interference.

Therefore, developments in bionanotechnology and the engineering of biological nanomachines allow communicating with biological systems at the molecular level by creating an interface between artificial or biological nanomachines and the neural network.

Our proposed scheme builds on extensive experiments/measurements carried out by the authors [25, 27, 31] and further develops the fascinating work of Nakano *et al.* [32] who proposed release-rate control schemes for DDS-based MC. The major contribution of the latter study was the proposal to assimilate MC into CNTs to optimise ACh conductivity in the artificial neural network. This approach improved the efficiency of neural signal transmission, as reported in [27]. Transmitter neurons (TNs) and receiver neurons (RNs) supported by a CNT-MEA biochip [25] show enhanced communication. Consequently, we propose a molecular switch, namely, a CNT-based XOR logic gate that allows fine-tuning of the TN ACh release rate according to the feedback concentration of ACh returned from the RN. To accomplish this, we exploited the design aspects of a neuron interface using a nanosensor [31] that is able to initiate neuronal signalling and that allows optimising the neuronal transmission-scheduling protocol. Subsequently, we used a Min/Max-based release-rate scheme that takes into account the ACh concentration and may work on top of the protocol to compensate for ACh transmission. In summary, the key goals of this study were as follows:

- To engineer an MC-based diffusion system in an artificial neural network to achieve the throughput and efficiency of molecular transmission.
- To integrate MC into CNTs exploiting the features of both CNTs and MC for optimising the performance of the artificial molecular nanonetwork.
- To use enzymatic kinetic theory to develop schemes to control the molecular release rate.
- To develop an susceptible-infected-recovered (SIR) epidemiological model of disease spreading.
- To analyse the performance of the nanonetwork in terms of mean delay delivery and incurred traffic rate.

The remaining of this paper is structured as follows. System descriptions, covering transmission, propagation, and reception processes in the engineered MC-based nanonetwork, are presented in Section 3; the applications of CNTs in nanomedicine are introduced in Section 4; the integration of CNTs and MC and the proposed min/max feedback control scheme are described in Section 5; the performance of the proposed nanonetwork is explored in Section 6; the results of numerical analysis performed through comparison are presented in Section 7; and in Section 8, we will draw valuable conclusions and delineate directions for future work.

3 Description of engineered MC system

This section introduces an engineered MC system for the proposed artificial neural nanonetwork, which includes synaptic transmission, diffusion, and enzyme kinetic reaction-based reception, as well as the derivation of upper-bound molecular transmission throughput.

3.1 Synaptic communication

In a nervous nanonetwork, neuronal communication is achieved at synapses, which are biological junctions through which the neural signal can be transferred between neurons or to other cells, such as muscle cells [33]. In other words, the synapse is the site of functional apposition between two cells, wherein the TN (i.e. presynaptic neuron) converts the electrical signal into a chemical signal that is released into the synaptic cleft to propagate and eventually bind to the receptors located on the membrane of the RN (i.e. postsynaptic neuron). As illustrated in Fig. 1, the neuron consists mainly of three functional parts: the soma (cell body), dendrites, and the axon. The electrical spike is generated from the soma only when the potential is above a threshold value. These spikes travel between the CNS and the various body parts. Dendrites and axons are outlets extending from the soma. The dendrites and soma allow the neuron to receive signals from other neurons, while the axons deliver the signal to other neurons. In this paper, a collection of neurons at the axon outlet called the nerve act as an intermediary node between the brain and the targeted cells. Thus, if any, damage occurs to the nerve, the communication between soma and target cells is interrupted, and the neuron is unable to effectively send the signal. Consequently, the CNS is able to control and connect other parts of the body through the neural circuits, which are formed by CNS synapses [16].

ACh is a natural neurotransmitter; it is part of the cholinergic nervous system and is responsible for high-level nervous activities, including learning, memory, and thinking [18, 35, 36]. The biological procedure associated with the synthesis, storage, receptor reaction, and termination of ACh has been summarised [37]. ACh molecules are mostly stored within vesicles, as shown in Fig. 1. An arrival AP at the presynaptic cell leads to ACh release based on 'a priori' probability. We modelled vesicle release as packet generation in the channel, which refers to converting the continuous spikes to the packet sequence in neuro-spike communication [5]. Therefore, ACh molecules are propagated by the presynaptic neuron in the synaptic cleft. Subsequently, the diffusion of ACh targeting the postsynaptic neuron is triggered. ACh molecules then bind to specific receptors on the target neuron via a receptor–ligand mechanism [34]. This binding opens an ion channel on the postsynaptic neuron, allowing the flow of ions into this neuron. We have investigated synaptic transmission and

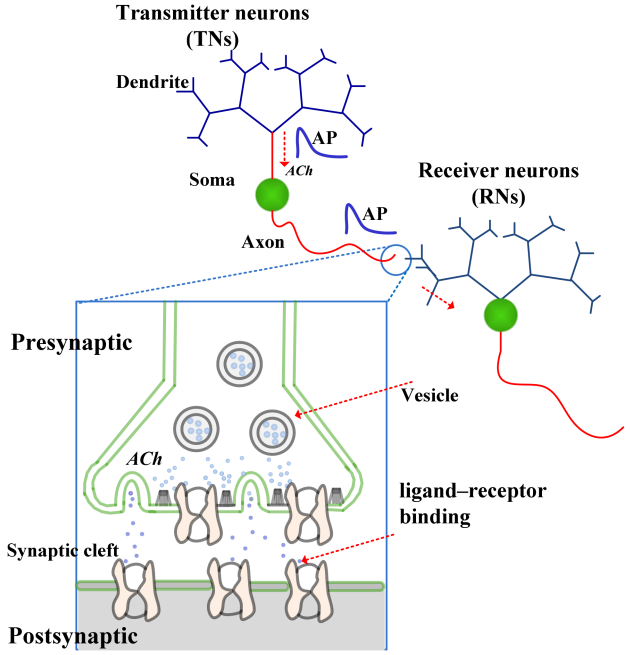

Fig. 1 *Synaptic communication*

information processing based on neuro-spike communication in neural networks in previous studies [5, 38, 39].

3.2 MC-based diffusion

We considered a nervous system sub-nanonetwork analogue of the intra-body nanonetwork proposed previously [15], which consists of a number of neurons that are able to collect and convey information between various parts of the nanonetwork. Communication between neurons starts when the APs travel from the presynaptic to the postsynaptic neurons via the synaptic cleft [40]. Consequently, a nanonetwork model is envisioned as communication between TNs and RNs, wherein the emission and reception of molecules act as communication signals. Furthermore, we envisaged the use of neurons cultured on a CNT substrate by means of nanotechnology to enhance neural connectivity and increase the efficacy of synaptic responses, as reported in [27].

To engineer a complete nanoscale MC nanonetwork for biological (bio-) nanomachines, we considered a simple hypothetical scenario comprising a number of bio-nanomachines, wherein N_n represents the number of nanocarriers. These bio-nanomachines carry ACh molecules in the proposed nanonetwork. Therefore, we use bio-nanomachines and ACh molecules interchangeably in this paper. For information transmission, the emission of ACh molecules takes place instantaneously via firing an AP spike, and thus, the TNs generate a number of ACh molecules with a release rate of R_{in} (molecules/s). Consequently, the molecular signal is encoded in different patterns of bursts of ACh molecules using simple ON/OFF keying (OOK) signalling or a binary symmetric Z channel [5]. Apart from the simplicity of the OOK scheme, it is appropriate for nanoreceiver design wherein ACh reception is similar to the closing or opening of the ion channel gate. We consider the size of the burst to be constant and equal to the transmission interval, T_{s}, which depends on the distance between the TN and RN and the location of the receptor on the RN.

We assumed the following: that the ACh molecules are transmitted in an aqueous medium; that the degradation rate of the ACh molecules (k_{d}) derives from a uniformly distributed in-body dynamic environment such as that caused by the presence of other molecules that react with ACh; pH; and environmental temperature and pressure. Furthermore, we assumed that ACh molecules circulate in adherence to Brownian motion and follow Fick's law of diffusion [32]

$$\frac{\partial C_{\text{ACh}}}{\partial t} = D\,\nabla^2 C_{\text{ACh}} - k_{\text{d}} C_{\text{ACh}} \tag{1}$$

where $C_{\text{ACh}}(x_1, x_2, \ldots, x_r, t)$ represents the concentration of ACh molecules as a function of time and r dimensions, D is the diffusion coefficient, and the Laplacian differential operator is

$$\nabla^2(.) = \frac{\partial^2(.)}{\partial x_1^2} + \frac{\partial^2(.)}{\partial x_2^2} + \cdots + \frac{\partial^2(.)}{\partial x_r^2}$$

for n dimensions.

Actually, we were interested in developing a closed-form expression for the steady-state ACh concentration, starting with $C_{\text{ACh}}(d, t)$ at distance d from the RN resulting in transmission and propagation. Therefore, we assumed all TNs to be at the origin of one-dimension ($r = 1$) and all RNs to be at location d (>0). Hence, the distance between the TNs and RNs is given as the average distance, d [32], and $C_{\text{ACh}}(d, t)$ is given by

$$C_{\text{ACh}}(d, t) = \frac{1}{\sqrt{4\pi D t}}\, \mathrm{e}^{-\left([\mu(t)]^2 + [\theta(t)]^2\right)} \tag{2}$$

where

$$\mu(t) = \frac{d}{\sqrt{4Dt}} \quad \text{and} \quad \theta(t) = \sqrt{k_{\text{d}} t}$$

MC occurs between groups of TNs and RNs, as illustrated in Fig. 2*a*, with each TN is capable of conveying ACh molecules that propagate in the medium. The receptors at the RN react chemically with the ACh molecules that diffuse through the medium and thus produce another type of molecule (P) in a process that is analogous to an enzyme kinetic process (i.e. ACh is a substrate/reactant and P is the reaction product). If the RN is not able to react fully, some of the ACh will remain in the medium and eventually degrade, thereby contributing to losses, as described later. Therefore, upon the transmission of an ACh burst, i.e. when every TN instantaneously transmits $R_{\text{in}} \times T_{\text{s}}$ molecules at the start of any independent time slot (T_{s}), the transmitted ACh diffuses in the medium by Brownian motion and may degrade at a fixed rate (k_{d}) as illustrated in (2). As a consequence, the contribution of ACh molecules transported at time jT_{s}, $j \in \{0, 1, 2, \ldots\}$ to the concentration monitored at distance d, denoted as $Q_j(d, t)$, is given by [32]

$$Q_j(d, t) = \begin{cases} N_n R_{\text{in}} T_{\text{s}} \times C_{\text{ACh}}(d, t - jT_{\text{s}}) & t \geq jT_{\text{s}} \\ 0 & t < jT_{\text{s}} \end{cases} \tag{3}$$

where N_n denotes the number of nanomachines carrying the information.

Fig. 2*b* illustrates the impact of (3), which indicates the degradation of ACh concentration over a long time (t) at different time slots (T_{s}) versus the separation distance (d) between the TN and RN. For an infinitesimal period δT_{s}, the ACh concentration at d and time $t = jT_{\text{s}}$ is the accumulation of all ACh molecules transmitted during 0–t, and can be expressed as follows:

$$\begin{aligned} Q(d, t) &= \lim_{T_{\text{s}} \to 0} \sum_{j=0}^{i} Q_j(d, t) \\ &= N_n R_{\text{in}} \lim_{T_{\text{s}} \to 0} \sum_{j=0}^{i} C_{\text{ACh}}(d, t - jT_{\text{s}}) T_{\text{s}} \\ &= N_n R_{\text{in}} \int_0^t C_{\text{ACh}}(d, T_{\text{s}}) \delta T_{\text{s}} \end{aligned} \tag{4}$$

Substituting (2) into (4), we obtain

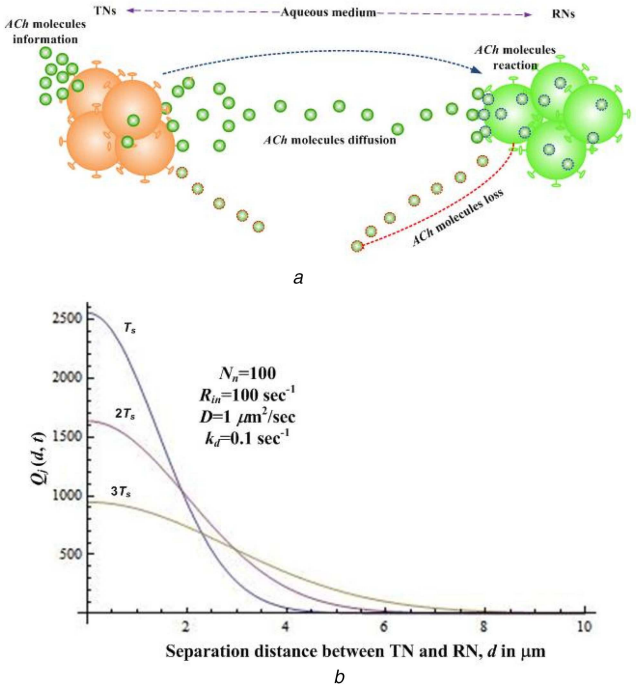

Fig. 2 *ACh MC-based neural network*
(a) Simplified system model, ***(b)*** Contribution of the transported ACh molecules at time slots T_{1-3}

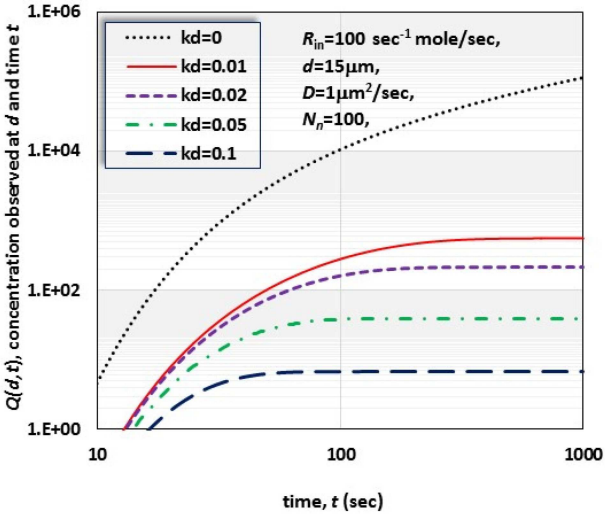

Fig. 3 *Concentration Q (d, t) in function of time (t) for various values of* k_d

$$Q(d,t) = N_n R_{\text{in}} \int_0^t \frac{1}{(4\pi\, D\, T_s)^{1/2}} e^{-((d^2/4DT_s)) + k_d T_s)} \delta T_s \tag{5}$$

An approximation solution of (5) is provided by Nakano *et al.* [32], as follows:

$$Q(d,t) \simeq N_n R_{\text{in}} \begin{cases} \left[\sqrt{\dfrac{t}{\pi D}} \times e^{-[\mu(t)]^2} - \dfrac{d}{2D}\, \text{erfc}(\mu(t))\right] & k_d = 0 \\ \dfrac{e^{-d\sqrt{k_d/D}}}{4\sqrt{k_d D}} \left[\begin{matrix} 2 - \text{erfc}(\theta(t) - \mu(t)) \\ -e^{2d\sqrt{k_d/D}} \times \text{erfc}(\theta(t) + \mu(t)) \end{matrix}\right] & k_d > 0 \end{cases} \tag{6}$$

Equation (6) reveals that the concentration $Q(d, t)$ depends mainly on the transmission rate R_{in} (molecules/s) and the number of bio-nanomachines (N_n) carrying the information. Moreover, it is a function of the system's parameters, such as degradation rate (k_d), diffusion coefficient (D), and average distance (d). We numerically solved (6) to determine the concentration $Q(d, t)$ at distance d and time t, as illustrated in Fig. 3, in which $Q(d, t)$ is plotted against the time t for different values of k_d and the indicated system's parameters. The effect of k_d on the transmitted concentration is obvious. After a sufficiently long time has elapsed ($t \to \infty$) from the point at which the TN begins conveying ACh molecules, the ACh concentration reaches the steady state. Therefore, by substituting $t \to \infty$ in (6), the steady-state concentration of ACh molecules at distance d resulting from the transmission process can be expressed in the following form:

$$Q(d) \simeq \begin{cases} \infty & k_d = 0 \\ N_n \times R_{\text{in}} \times \dfrac{e^{-d\sqrt{k_d/D}}}{2\sqrt{k_d D}} & k_d > 0 \end{cases} \tag{7}$$

3.3 Reception process

The reception process occurs via a ligand–receptor mechanism. As described above, ACh is responsible for synaptic transmission; thus, ACh, acting as the ligand, activates the receptor, thereby establishing the ligand–receptor mechanism. We assumed the postsynaptic neuron to have a number N_r of postsynaptic receptors (e.g. nicotinic receptors), each having a volume v. ACh is enzymatically hydrolysed into choline and acetic acid by acetylcholinesterase (AChE) in the synapse, and the enzymatic activities are mostly expended on incoming ACh. However, synaptic transmission in a nervous nanonetwork may be disrupted by nerve agents, which are organophosphate chemicals that inhibit AChE [41]. This means that AChE inhibitors relax the degradation rate and permit more ACh to bind to the postsynaptic receptors. Therefore, we exploit enzyme kinetics theory to obtain a closed-form expression for the upper-bound throughput as illustrated in (13).

At the moment, we expressed the overall reaction rate by multiplying the receptor volume, v and the chemical reaction rate, $\Omega(.)$ (which is effectively a function of ACh concentration at distance d) in the steady state at the RN as $R_{\text{out}}(d)$:

$$R_{\text{out}}(d) = \nu \Omega(C_{\text{ACh}}(d)) \tag{8}$$

The ACh molecules bind to the receptors on the RN surface and are transformed into bound complexes P through a series of steps analogous to the enzymatic reaction. Subsequently, ACh is released according to the reverse binding rate (k_r), and its chemical formulation depends on the forward binding rate (k_f) according to reaction kinetics. This reaction is expressed as [42]

$$\text{ACh} + E \underset{k_r}{\overset{k_f}{\longleftrightarrow}} C \to P + E \tag{9}$$

where ACh and E (i.e. ACh receptors on the RNs) interact to form a complex C (ACh–E). C is separated into ACh and E or is converted to P (product) and E. Therefore, the chemical reaction rate at the RN for only one binding site, $\Omega(C_{\text{ACh}})$ (the number of ACh molecules reacting per unit volume) can be expressed as a hyperbolic function [43]

$$\Omega(C_{\text{ACh}}) = \frac{V_{\max} \times C_{\text{ACh}}}{V_{1/2} + C_{\text{ACh}}} \tag{10}$$

where $V_{\max}$ is the maximum reaction rate and $V_{1/2}$ is half the ACh concentration. Notably, the chemical reaction rate, $\Omega(C_{\text{ACh}})$ for a receptor with multiple binding sites (n) can be expressed by a sigmoidal function as follows:

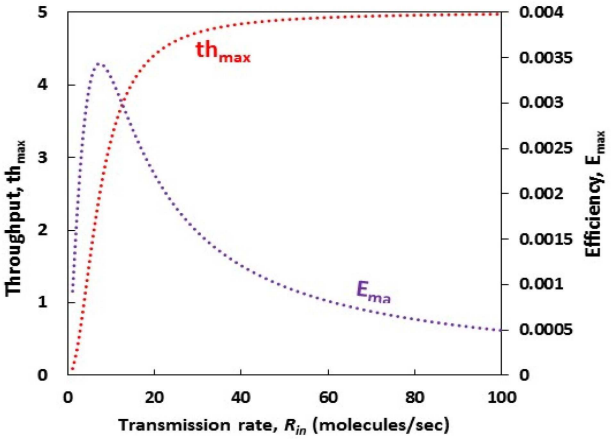

Fig. 4 *Transmission throughput and efficiency of ACh in the proposed nanonetwork*

$$\Omega(C_{\mathrm{ACh}}) = \frac{V_{\max} \times (C_{\mathrm{ACh}})^n}{(V_{1/2})^n + (C_{\mathrm{ACh}})^n} \tag{11}$$

After the ACh molecules have been recognised by a postsynaptic receptor, some are propagated back into the synaptic cleft [17]. Therefore, we were interested in evaluating the number of ACh molecules that react with the receptors per unit time (defined as throughput). The steady-state transmission reveals that $Q(d)$ in (7) is equal to or larger than the $C_{\mathrm{ACh}}(d)$ (i.e. $Q(d)C_{\mathrm{ACh}}(d)$). Therefore, $\Omega(C_{\mathrm{ACh}})$ in (11) is an increasing function, and can be used to develop an expression for the upper-bound throughput, $\mathrm{th}_{\max}$ [32]

$$\mathrm{th}_{\max} \cong \sup\{\nu \times N_{\mathrm{r}} \times \Omega(C_{\mathrm{ACh}}(d))\} = \sup\{\nu \times N_{\mathrm{r}} \times \Omega(Q(d))\} \tag{12}$$

Using (11) and (7), the upper-bound throughput ($\mathrm{th}_{\max}$) in (12) is deduced as

$$\mathrm{th}_{\max} = \frac{\nu \times N_{\mathrm{r}} \times V_{\max} \times (N_n \times R_{\mathrm{in}})^n}{\left(2\sqrt{k_{\mathrm{d}}D} \times V_{1/2} \times \mathrm{e}^{d\sqrt{k_{\mathrm{d}}/D}}\right)^n + (N_n \times R_{\mathrm{in}})^n} \tag{13}$$

Furthermore, the transmission efficiency (E) can be computed by dividing $\mathrm{th}_{\max}$ by the total number of transmitted ACh molecules per unit time. Supplementary to the previous calculation, the upper-bound efficiency ($E_{\max}$) is given as

$$E_{\max} \cong \frac{\mathrm{th}_{\max}}{N_n \times R_{\mathrm{in}}} \tag{14}$$

It is important to calculate throughput and ACh transmission efficiency because ACh plays a crucial role in the peripheral nervous system during muscle movement and in the CNS, where it is believed to affect learning and memory [18, 35, 36]. As a consequence, throughput and efficiency are considered promising pharmacological measures of ACh molecule transmission, especially in DDSs. We numerically solved the above equations to show the performance of transmission throughput and efficiency versus the transmission rate (R_{in}), as illustrated in Fig. 4. We found that the transmission throughput increased as the transmission rate increased, and the transmission efficiency was very sensitive to the transmission rate, especially at low values. Interestingly, the efficiency of the ACh molecules was in accordance with previous results on spike (AP) performance in MC-based artificial neural networks [31] and clustered neurons in CNTs [27].

3.4 Propagation analysis

We have previously studied a paradigm for MC among nanomachines based on a collision/adhesion mechanism [5]. We proved that, upon collision, adhesion is accomplished, allowing information exchange between nanomachines. Successful transmission is achieved using the neuro-spike communication paradigm [5]. In the proposed system model, we applied a propagation model comprising a single packet of information generated by the TN, which is used to model the distribution of an infectious disease. In epidemic disease-spreading schemes based on the standard SIR model [5], a single packet is propagated in accordance with the discipline of store-carry-forward. In this context, we consider the single packet of information to be analogous to the ACh molecule, which is released from a vesicle. Moreover, in the proposed network, ACh propagation is affected by various environmental factors, such as pH, temperature, the viscosity of the medium, and the distance between the TN and the RN [20, 32]. Therefore, we should take into account the interaction of the ACh molecules at the RN, i.e. maximum transmission throughput ($\mathrm{th}_{\max}$).

As previously mentioned, we denoted the total number of bio-nanomachines as N_n; their purpose is to carry the ACh molecules in the nanonetwork. Furthermore, T_{d} is a random variable defined as the time elapsed from the release of the ACh molecule by the TN until the time point at which the packet is received by the RN. Aligned to the SIR model [5], $s(t)$, $i(t)$, and $r(t)$ represent the number of suspected nanomachines, the number of infected nanomachines, and the number of recovered nanomachines at time t, respectively. Hence, the transition rate into state i can be deduced as $\beta \times s \times i$, whereas the transition rate escaping from a state i yields $\gamma \times i$. β stands for the rate of packet spread among nanomachines with a transmission throughput $\mathrm{th}_{\max}$, and γ indicates the rate with a transmission throughput $\mathrm{th}_{\max}$ at which infected nanomachines are recovered. Furthermore, we adopted the MAMNET paradigm and previous findings [5, 44] as part of the propagation process to evaluate the parameters β and γ by taking into account ACh transmission throughput as follows:

$$\beta = \begin{cases} (C_{\mathrm{nn}} \cdot P_{\mathrm{a}} \cdot P_{\mathrm{t}}) \times \mathrm{th}_{\max} & t > 0 \\ 0 & t = 0 \end{cases}$$
$$\text{and} \tag{15}$$
$$\gamma = \begin{cases} (C_{\mathrm{ni}} \cdot P_{\mathrm{a}} \cdot P_{\mathrm{t}}) \times \mathrm{th}_{\max} & t > 0 \\ 0 & t = 0 \end{cases}$$

where C_{ni} and C_{nn} denote the collision rate for nanomachine and infected nanomachine, and the collision rate between two nanomachines, respectively. P_{a} and P_{t} represent the probability of adhesion and the probability of successful transmission, respectively. The extrapolated expressions for these parameters have been derived based on the molecular electronic structure of the ACh neurotransmitter and the parameters of a neuro-spike communication system [5].

4 CNTs in nanomedicine applications

CNTs are an emerging nanomaterial entirely composed of carbon atoms arranged as benzene rings. The rings are combined with graphene sheets that are rolled up to formulate smooth cylinders. There are two main types of CNTs: single-walled and multi-walled, both of which have been investigated intensively [45]. CNTs are usually synthesised in function of the desired structure and application. Their chemical and physical characteristics, such as high aspect ratio and high electrical/thermal conductivity, make CNTs useful for applications in nanomedicine.

New uses for CNTs in the field of bionanotechnology have recently emerged. The use of CNTs for disease detection and therapy has raised high expectations. Consequently, CNTs constitute attractive solutions for neuroscience and tissue engineering, especially neuronal and ligamentous tissue growth for CNS regenerative interventions (e.g. brain and spinal cord) and orthopaedic purposes [46]. Moreover, CNTs can be utilised as components of ion channel blockers and protein and DNA biosensors in parallel with bioseparators and biocatalysts [32]. Furthermore, the surfaces of CNTs can be modified with a nanomaterial coating, heralding the next generation of biosensors

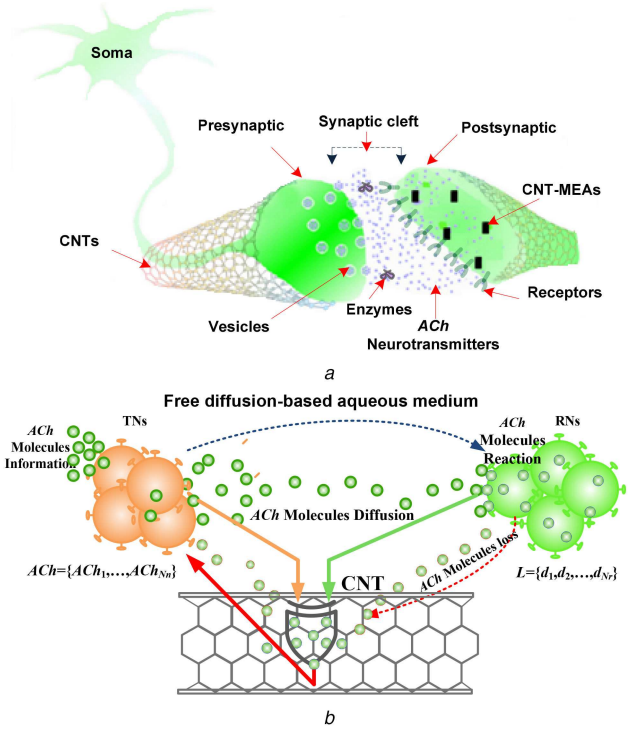

Fig. 5 *Proposed nanonetwork incorporating MC and CNTs*
(a) Cultured neural network-based CNT, ***(b)*** Graphical illustration of the proposed scheme

and bioelectronic devices utilised in biomedical applications and enhancing the performance of existing nanotechnologies [47]. Moreover, molecular transportation systems based on the chemical interaction between the CNT wall and the molecule encapsulated in the CNT or on translocation across the cell membrane and solubilisation have been designed [48, 49]. Experimental results [50] have revealed the usability of single-walled CNTs as carriers in pharmacological formulations for the treatment of peptic tract diseases as well as the successful integration of CNTs with biomolecules. The incorporation of biomolecules within CNTs permits their use in hybrid communication systems as active field-effect transistors and electrochemical biosensors (enzymatic, DNA sensors, or immune-sensors). Furthermore, a nanomachine to fulfil the basic functions of a biological synapse in a neural network has been fabricated [51]. Accordingly, CNTs have been used in intra-body nervous systems to probe and track cell behaviour and to enhance the tissue matrix [51].

5 Integrating MC and CNTs

The main goal of this study was to shed light on the integration of MC and CNTs to enhance the performance of intra-body nanonetwork, such as the nervous system. We exploited MC technology and the features of CNTs to propose an assimilation scheme. The proposed scheme enables increasing or decreasing signalling transmission between the TNs and RNs by using MC among nanomachines. Additionally, neuron ends are equipped with a CNT-MEA chip for wireless interconnection purposes to achieve reliable communication between two neurons. At the molecular level, we envision CNTs are embedded within an XOR gate to act as a switch to control the concentration of transmitted molecules. To accomplish this, we propose min/max feedback control schemes for adjusting the transmission rate in the intra-body nervous system nanonetwork.

5.1 Proposed scenario: assimilation scheme

In neural networks, the brain alters the activity of the neurons using neurotransmitters; therefore, communication between presynaptic (i.e. TN) and postsynaptic (i.e. RN) neurons is managed by synaptic transmission. Furthermore, neurons are able to regulate synaptic activity using autoreceptors on the presynaptic neuron that sense the number of neurotransmitters in the communication channel (i.e. cleft); if there is an excessive number, the presynaptic neuron decreases the release rate [52]. Similarly, postsynaptic receptors use this regulation process as follows: when the release rate of the neurotransmitter is unusual, postsynaptic receptor sensitivity or numbers are changed to compensate. Unbound neurotransmitters may remain in the cleft channel and are not efficiently taken up, resulting in communication failure across a synapse. Moreover, some enzymes abrogate such neurotransmitter accumulation and hyper-stimulation, thereby influencing the release rate, and may be involved in diseases that affect the intellect [17]. Based on the mechanism of synaptic activity regulation, we propose a new scheme for enhancing MC in neural networks using CNTs, building on recent findings [25, 27, 31]. Further, we envisaged the proposed MC to enable increased and decreased signalling in neural networks.

As illustrated in Fig 5*a*, we consider a neural network to consist of neurons cultured on a CNT substrate in which MC takes advantage of the favourable features of the CNTs. The presynaptic and postsynaptic neurons are equipped with a CNT-MEA chip for wireless interconnection purposes to achieve reliable communication. The CNT-MEA approach is considered to be non-invasive and enables the sensors to interface with the neurons, thereby activating signalling between the TNs and RNs. Consequently, we propose a min/max feedback control schemes to adjust the release rate of neurotransmitters as explained in the following subsection.

5.2 Release rate-based min/max scheme

The ACh neurotransmitter molecules are released from the TN and diffuse across the synaptic cleft (the communication channel) to the RN in the nervous nanonetwork. However, a loss of synaptic communication may occur because some of these molecules are lost or remain in the channel, or may be affected by enzymes (e.g. ACh is hydrolysed by AChE). Many approved drugs take advantage of this mechanism to tackle diseases such as Alzheimer's disease and myasthenia gravis. Alzheimer's disease damages ACh receptors, resulting in memory loss, mood swings, and language degeneration, and hence, it reduces the ability of the nervous nanonetwork to enhance ACh transmission. Inspired by chemical-reaction and enzyme kinetics, we mimicked this scenario according to the system model of MC and the determination of molecular transmission throughput in Section 3. We assumed that the RN produces a feedback of ACh molecules, namely $\mathrm{ACh_{fb}}$, which refers to lost molecules. This occurs in parallel with RN action, which may break the chemical bond with a feedback reaction rate, $\Omega([\mathrm{ACh_{fb}}])$, to produce free $\mathrm{ACh_{fb}}$ molecules in the communication channel. This chemical process can be described as follows [32]:

$$\mathrm{ACh} \times \mathrm{ACh_{fb}} + E \underset{k_r}{\overset{k_f}{\longleftrightarrow}} \mathrm{ACh} \times \mathrm{ACh_{fb}} \times E \rightarrow P + E + \mathrm{ACh_{fb}} \quad (16)$$

The feedback ACh molecules may remain in the communication channel and will probably degrade, resulting in a loss of ACh molecules. Consequently, the efficiency of ACh transmission and its throughput in the nervous system mainly depend on the feedback concentration of ACh that is released from the RN [32]. This affects the ACh propagation and diffusion. Thereafter, the transmission rate to the postsynaptic neuron is directly affected. According to the transmission rate control for MC, which exploits the positive and negative feedback schemes [32], we aimed to develop a new ACh release-rate scheme by incorporating CNTs and MCs in the proposed nanonetwork, exploiting wireless CNT-MEA technology. A CNT-MEA at the postsynaptic neuron (RN) enables the presynaptic neuron (TN) to control the number of neurotransmitters according to the feedback activities of ACh. Therefore, our goal was to model MC between the TNs and RNs based on artificially induced CNTs.

To accomplish this, we employed design aspects [31] that activate the neuron interface using a nanosensor that is able to

initiate neuronal signalling and allows optimising the transmission between neurons. Subsequently, we proposed a min/max-based release-rate scheme that is aware of ACh concentration, which may work on top of this protocol. Analogous to communication networks, a buffer overflow may happen at the receiver node if the transmitter node sends packets at a rate higher than the reception rate. In the schemes we propose, min and max schemes are analogous to negative feedback and positive feedback control. We assumed that the feedback concentration is always high, referring to buffer overflow. As a consequence, in the Min scheme, TN decreases the release rate as opposed to the max scheme, which increases the release rate. By adopting the transmission rate, the max scheme can achieve the expected efficiency while the min scheme can maintain the throughput.

Consequently, in the min-based scheme, the TN decreases the release rate when the feedback ACh concentration is high. In other words, it decreases the release rate of ACh and alleviates throughput increase, $\text{th}_{\max}$ (13), and thus sustains the expected throughput. In contrast, in the max-based scheme, the TN increases the release rate when the back-propagation ACh concentration is high. Alternatively, the transmission rate increase leads to an increase in throughput and efficiency. Furthermore, $E_{\max}$ is calculated by dividing $\text{th}_{\max}$ by the transmission rate (14), and thus the max-based scheme can achieve the expected efficiency by fine-tuning the ACh concentration. To illustrate the proposed scheme, we described the CNTs as acting as an XOR-switch between TNs and RNs, as portrayed in Fig. 5*b*. Accordingly, the TN is able to adopt a release rate based on the concentration of the feedback ACh molecules at the TN location ($d = 0$) and time t as follows: $R_{\text{in}} = \nu \times \Omega([\text{ACh}_{\text{fb}}(0, t)])$ .We modelled the feedback concentration of ACh molecules by applying enzyme kinetic theory and adopting the findings of Nakano *et al.* [32] for positive and negative feedback schemes in order to utilise the transmission rate (R_{in}) of ACh. We denoted the feedback concentration as ACh_{fb}, and the feedback molecules that react with the TNs were defined as $\Omega([\text{ACh}_{\text{fb}}])$. Using the derived expression of feedback reaction [32], $\Omega([\text{ACh}_{\text{fb}}])$ can be expressed as follows:

$$\Omega([\text{ACh}_{\text{fb}}]) = \begin{cases} \dfrac{Y_1 \cdot X_1}{Y_1 + [\text{ACh}_{\text{fb}}]} + Z_1 \text{ for min} - \text{based scheme} \\ \dfrac{X_2 \cdot [\text{ACh}_{\text{fb}}]}{Y_2 + [\text{ACh}_{\text{fb}}]} + Z_2 \text{ for max} - \text{based scheme} \end{cases} \tag{17}$$

where X_1, X_2, Y_1, and Y_2 are the coefficients associated with reactions among TNs and ACh feedback molecules. Z_1 and Z_2 are leakage rate constants [32].

Consequently, we envisioned a simple yet meaningful scenario whereby the CNTs are embedded within the XOR gate and implemented at the molecular level by pseudorotaxane [53]. This scenario involves the chemical reaction and feedback reaction rates of ACh. We were inspired by the development of the CNTs-MEA chip [25] and design aspects of a neuron interface-based nanosensor [31] in a cultured neural network, which is non-invasive and enables the measurement of neurotransmitter activities at both presynaptic and postsynaptic neurons. It is possible to envision the two inputs of the XOR gate as ACh and ACh_{fb} concentrations, and we denoted the output of XOR as I_{ACh}. Therefore, the output of the XOR gate is capable of inducing the TN to minimise or maximise the release rate (R_{in}) and ACh concentration at the next transmission interval, as follows:

$$I_{\text{ACh}} = \text{ACh}_{\text{fb}} \oplus \text{ACh} \tag{18}$$

To fulfil this scenario, we used ACh concentration in the OOK scheme. Notably, ACh at low concentrations is expressed as binary information (bit 0), whereas high concentration is expressed as bit 1. Furthermore, invoking the scenario of the min/max-based scheme, we acknowledged the feedback concentration of ACh_{fb} to be high (worst scenario) and thus, I_{ACh} was constantly computed as $I_{\text{ACh}} = 1 \oplus \text{ACh}$. Consequently, when the concentration of ACh is low (i.e. 0), $I_{\text{ACh}} = 1$ and the CNT-based XOR output induces the TN to increase ACh release in the next time slot to compensate for the expected efficiency by fine-tuning the transmission rate and concentration. Conversely, when the concentration of ACh is high (i.e. 1), $I_{\text{ACh}} = 0$. Thus, the CNT-based XOR output forces the TN to reduce ACh release in the next time slot to attain the expected throughput.

6 Performance analysis of the proposed nanonetwork

In this section, we present the performance evaluation of the proposed nanonetwork-based min/max schemes. To accomplish this goal, we investigated the performance of the nanonetwork by adopting the MAMNET concept [44] while taking into account the expected value of $\text{th}_{\max}$ at the RN. Moreover, the transmission rate in the context of MAMNET is realised through three tractable phases: collision, adhesion, and successful transmission probability in terms of spreading (β) and recovery rate (γ). Consequently, we analysed performance metrics such as average packet delay, throughput, and incurred traffic rate during the application of the proposed min/max-based scheme. The average packet delay $E[T_{\text{d}}]$ necessitated effective delivery of nanoscale packet information from TNs to RNs, and is expressed as follows [5]:

$$E[T_{\text{d}}] = \int_0^{\infty} (1 - F(t))\text{d}t = \int_0^{\infty} \left(1 - \frac{1}{N_n}\right)^{-\gamma/\beta} \times \left[1 - \frac{4\pi\left(r_i^3 - r_n^3\right)}{3V}\right] \left(\frac{N_n - 1}{[N_n - 1] + \text{e}^{\beta N_n t}}\right) \text{d}t \tag{19}$$

where r_n and r_i denote the radii of the bio-nanomachine and the RN receptors, respectively. Using a hypergeometric function ${}_2^0\mathcal{F}_1\{a; b; c; z\}$, $E[T_{\text{d}}]$ is calculated as follows [54]:

$$E[T_{\text{d}}] = \frac{(N_n)^{\frac{\gamma}{\beta}-1}}{2\gamma} \left[1 - \frac{4\pi\left(r_i^3 - r_n^3\right)}{3V}\right] \times {}_2\mathcal{F}_1\left\{\frac{\gamma}{\beta}; \frac{\gamma}{\beta}; 1 + \frac{\gamma}{\beta}; N_n - 1\right\} \tag{20}$$

The average throughput (η) for sending b bits of ACh is given by

$$\eta = \frac{b}{E[T_{\text{d}}]} \tag{21}$$

Additionally, the average incurred traffic rate (ρ_{itr}) for sending b bits of ACh to RN is given by [5]

$$\rho_{\text{itr}} = \frac{N_n \times \eta}{1 + (N_n - 1)\text{e}^{-\beta N_n E[T_{\text{d}}]}} \tag{22}$$

7 Numerical results

In this section, we present the performance analysis of the proposed nanonetwork based on MC and CNT nanotechnology. We have divided this section into two subsections. In the first subsection, we numerically evaluated the throughput ($\text{th}_{\max}$) and efficiency ($E_{\max}$) resulting from ACh transmission, propagation, and chemical reaction processes. $\text{th}_{\max}$ and $E_{\max}$ were computed in terms of the release rate R_{in} [(13) and (14)]. These equations take into account default parameters for this designated scenario, which are listed in Table 1.

In the second subsection, we analyse the performance of the proposed nanonetwork utilising the min/max-based release-rate scheme and we compare the performance of the min/max-based release-rate schemes with a static scheme, for a fixed release rate. Because they occur naturally in biochemical neural systems, we employed the typical parameters described in the literature [5, 32] in our simulation. We used Matlab software code for simulations and adopted the default parameters listed in Table 1 [5].

Table 1 Default parameters for simulations

Parameter	Value
number of nanomachine receivers, N_r	5
number of nanomachines, N_n	10–100
volume, v	0.1 μm^3
diffusion coefficient, D	1 $\mu m^2/s$
maximum reaction rate, V_{max}	10 $\mu m^{-3}/s$
half of ACh concentration, $V_{1/2}$	10 μm^{-3}
decay rate of ACh molecules, k_d	0.1 s^{-1}
number of binding sites, n	1–5
number of bits, b	8 bits
release rate, R_{in}	0–100 s^{-1}

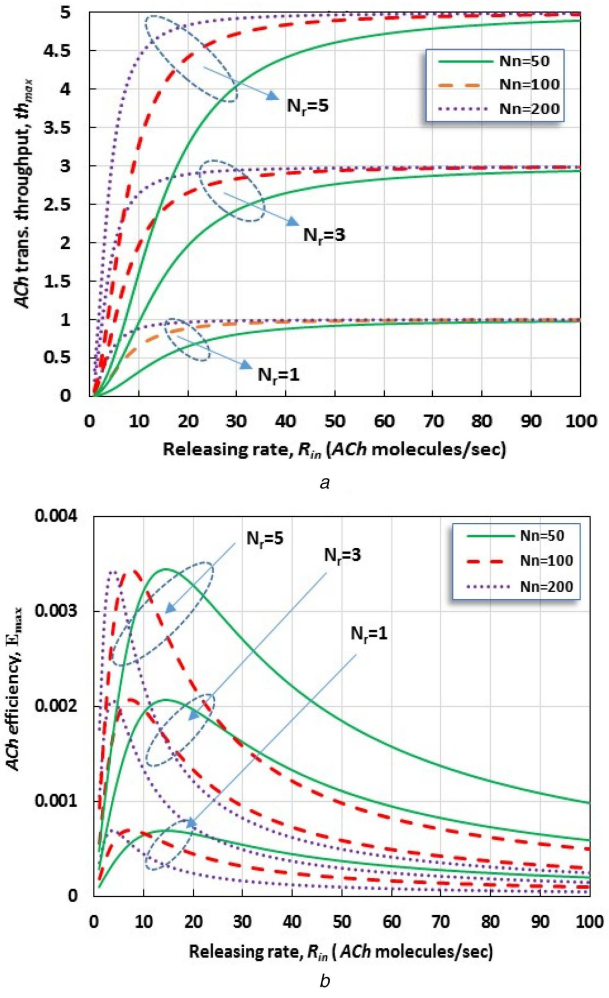

Fig. 6 *ACh transmission performance*
(a) th_{max} against R_{in}, ***(b)*** E_{max} against R_{in}

7.1 ACh transmission throughput and efficiency

Figs. 6*a* and *b* show the throughput (th_{max}) and efficiency (E_{max}) of the ACh molecules as the release rate (R_{in}) increased from 0 to 100 s^{-1} for different numbers of receptors (N_r) and (N_n) of nanomachines, respectively. As expected, both th_{max} and E_{max} increased in value as N_r and N_n increased, respectively. Notwithstanding, the principal observation from these figures is the influence of R_{in} on both th_{max} and E_{max}.

As demonstrated, th_{max} rose as R_{in} increased. Notably, when R_{in} was relatively high, the ACh concentration at the RN was raised, and the reaction rate at the RN was relatively high. E_{max} increased when R_{in} increased from 0 until it peaked and then gradually diminished to 0. Therefore, increasing R_{in} leads to chemical reaction saturation at the RN, and a consequent deterioration of E_{max}.

We can conclude that, when the release rate R_{in} is sufficiently high, the absorption of ACh molecules (i.e. concentration) at the RN is sufficiently high to sustain the maximum reaction rate, i.e. the upper-bound limit of expected throughput (13) is fulfilled. On the other hand, according to (14), the upper-bound limit of expected efficiency is a decreasing function of R_{in}. This association between th_{max} and E_{max} enables us to determine accurately the optimal transmission rate in such a nanonetwork.

7.2 Performance of the proposed nanonetwork

We analysed the performance of the proposed nanonetwork based on the min/max schemes. For comparison purposes, we investigated the performance of the proposed nanonetwork scenario for a static release rate of ACh, namely the static scheme. In that case, the steady-state concentration is obtained with (7). The default parameters are shown in Table 1. We investigated two scenarios as illustrated in the following subsections.

7.2.1 Effects of environmental parameters: In this scenario, we evaluated the performance of ACh throughput (th_{max}) as a function of the diffusion coefficient D and the degradation rate k_d, which represent the environmental parameters under the proposed scheme. The aim was to illustrate the effects of environmental parameters on ACh transmission throughput. As depicted in Figs. 7*a* and *b*, as D increased, th_{max} responded in an analogous manner (concave upward curve), whereas th_{max} decreased as k_d increased (concave downward curve) for each examined simulation. Notably, small values of D entail limited movement of ACh molecules in the environment and a limited number of ACh molecules being received by the RN (i.e. low th_{max}) as a result of an environmental impediment. Large values of D lead to a th_{max} increase when the diffusivity of ACh molecules in the medium is high. Physically, by observing k_d caused by the reaction of ACh molecules with other molecules, blood pressure, and environmental temperature, we concluded that th_{max} peaks when the effects of these parameters are limited. It is possible to trace the results for the static scheme between the min and max-based schemes. Additionally, the min-based scheme attained a higher level of throughput than the max-based scheme, which is explained by the fact that the decrease in the release rate of ACh prevents a further increase in throughput, and sustains the expected throughput.

In addition, the graphs reveal that the proposed schemes may be adopted to release the ACh molecules according to environmental conditions. For instance, assuming a static channel or environment, the design of bio-nanomachines may be engineered with the sole goal to transmit ACh molecules at the optimal transmission rate, while in a dynamic environment, such optimisation is externally steered. In fact, the integration of MC and CNTs favours the autonomous optimisation by bio-nanomachines, adjusting the transmission rate according to environmental conditions.

7.2.2 Metrics performance of proposed nanonetwork: In this scenario, we evaluated the network performance metrics such as average packet delay, throughput, and incurred traffic rate of the proposed nanonetwork, as illustrated in Figs. 8*a–c*. The default parameters for this scenario are depicted in Fig. 8. The average packet delay $E[T_d]$ for ACh transmission is shown in Fig. 8*a*. The min-based scheme superseded the max-based scheme because the number of ACh molecules proceeded by the RN per unit time was high, assuming the min-based scheme was employed, and thus, the expected throughput was achieved. This led to a decrease in the average delay of ACh delivery as compared to the static and max-based schemes. Decreasing the time delay for ACh delivery to the RN produced a high nanonetwork throughput and incurred traffic, as shown in Figs. 8*b* and *c*, respectively. This is because the average number of ACh received by the RN is proportional to the delay in ACh delivery. In other words, the shorter the delay, the higher the throughput and incurred traffic.

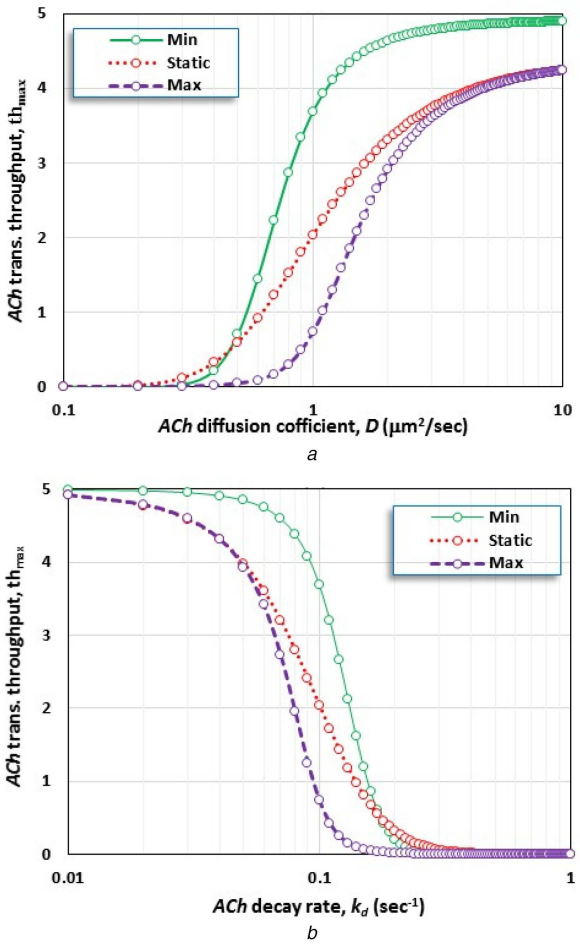

Fig. 7 *Throughput comparison-based system parameters*
(a) $\mathrm{th}_{\max}$ against D, ***(b)*** $\mathrm{th}_{\max}$ against k_{d}

In summary, our analysis illustrates that the network performance metrics in terms of transmission throughput, average time delay, and incurred traffic can be evaluated based on the proposed feedback control schemes that enable bio-nanomachines to adopt the release rate according to the feedback molecules released from the RN caused by chemical reaction with ACh molecules transmitted from the TN. On the other hand, the variance of nanonetwork throughput and efficiency in a dynamic environment can be managed by deploying the Min and Max feedback control schemes. Additionally, the MC-CNT assimilation scheme can maintain the robustness of the nanonetwork against environmental variations including pH level and temperature.

8 Conclusions

Optimising ACh molecule conductivity in neural nanonetwork could provide improved nanomedical systems that are potentially useful in the treatment of chronic health conditions. Furthermore, the proposed nanonetwork, which was investigated in terms of average transmission throughput, average time delay, and acquired traffic rate, paves the way for ICT-inspired detection/diagnosis and innovative medical techniques. On that basis, the current work could lay the foundation for future work in nanomedicine, leading to the alleviation or even treatment of neurodegenerative diseases. Therefore, such nanonetwork could be used in brain–machine interfaces in the near future.

9 Acknowledgment

The authors extend their appreciation to the Deanship of Scientific Research at King Saud University for supporting this work through research group no (RGP-1438-27).

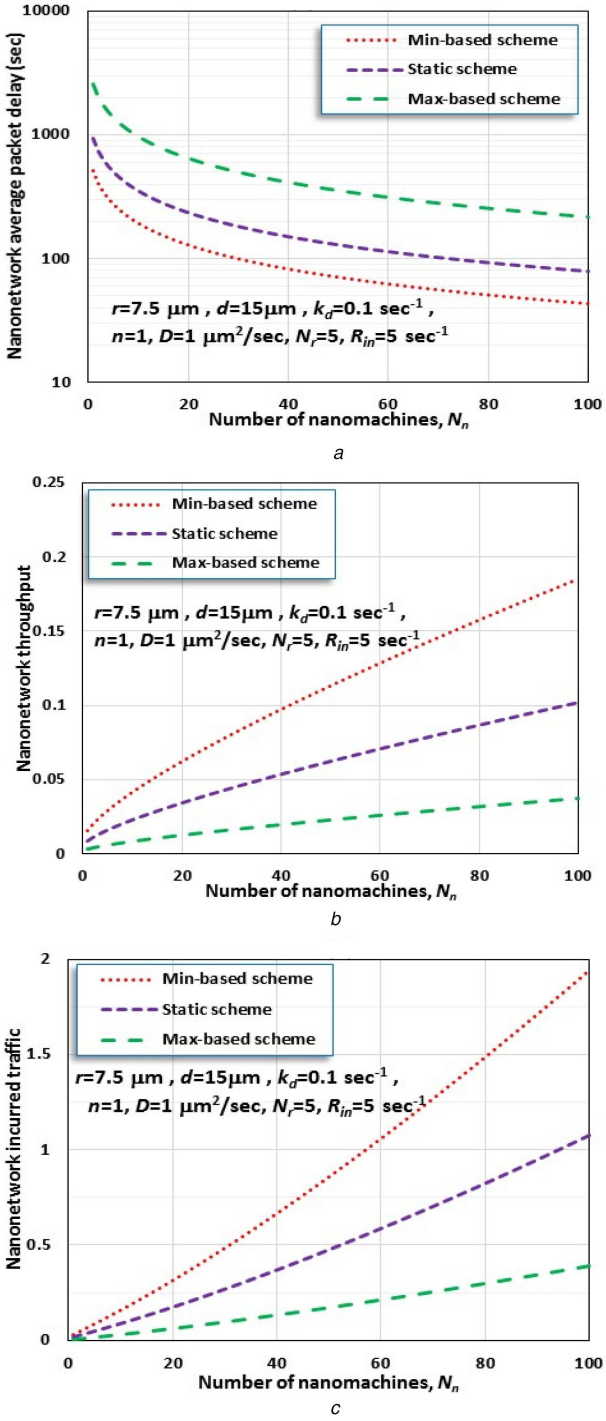

Fig. 8 *Nanonetwork performance metrics*
(a) $E[T_{\mathrm{d}}]$ against N_n, ***(b)*** $\mathrm{th}_{\max}$ against N_n, ***(c)*** ρ_{itr} against N_n

10 References

[1] Madani, S.Y., Naderi, N., Dissanayake, O., *et al.*: 'A new era of cancer treatment: carbon nanotubes as drug delivery tools', *Int. J. Nanomed.*, 2011, **6**, pp. 2963–2979

[2] Suda, T., Moore, M., Nakano, T., *et al.*: 'Exploratory research on molecular communication between nanomachines'. Proc. Genetic and Evolutionary Computation Conf. (GECCO'05), June 2005, pp. 1–4

[3] Akyildiz, I.F., Brunetti, F., Blazquez, C.: 'Nanonetwork: a new communication paradigm', *Comput. Netw.*, 2008, **52**, pp. 2260–2279

[4] Nakano, T., Eckford, A., Haraguchi, T.: '*Molecular communication*' (Cambridge University Press, Cambridge, UK, 2013)

[5] Abd El-atty, S.M., Gharsseldien, Z.M., Lizos, K.A.: 'Framework for single input single output nanonetwork-based realistic molecular communication', *IET Nanobiotechnol.*, 2015, **9**, (6), pp. 331–341

[6] Farsad, N., Yilmaz, H.B., Eckford, A., *et al.*: 'A comprehensive survey of recent advancements in molecular communication', *IEEE Commun. Surv. Tutor.*, 2016, **18**, (3), pp. 1887–1919

[7] Felicetti, L., Femminella, M., Reali, G., *et al.*: 'Applications of molecular communications to medicine: a survey', *Nano Commun. Netw.*, 2016, **7**, pp. 27–45

[8] Chahibi, Y.: 'Molecular communication for drug delivery systems: a survey', *Nano Commun. Netw.*, 2017, **11**, pp. 90–102

[9] Minnikanti, S., Peixoto, N.: 'Implantable electrodes with carbon nanotube coatings', in Marulanda, J.M. (Ed.): '*Carbon nanotubes applications on electron devices*' (InTech, NewYork, 2011), ch. 6

[10] Cipollone, S.: 'Carbon nanotubes and neurons: nanotechnology application to the nervous system', PhD thesis, Universitá degli Studi di Trieste, 2009

[11] Guo, X., Small, J.P., Klare, J.E., *et al.*: 'Covalently bridging gaps in single-walled carbon nanotubes with conducting molecules', *Science*, 2006, **311**, (5759), pp. 356–359

[12] Qian, H., Lu, J.-Q.: 'Molecular electronic switch using carbon nanotube electrodes', *Phys. Lett. A*, 2007, **371**, pp. 465–468

[13] Abidian, M.R., Kim, D.-H., Martin, D.C.: 'Conducting-polymer nanotubes for controlled drug release', *Adv. Mater.*, 2006, **18**, (4), pp. 405–409

[14] Zhang, W., Zhang, Z., Zhang, Y.: 'The application of carbon nanotubes in target drug delivery systems for cancer therapies', *Nanoscale Res. Lett.*, 2011, **6**, pp. 555. doi: 10.1186/1556-276X-6-555

[15] Malak, D., Akan, O.B.: 'Communication theoretical understanding of intra-body nervous nanonetworks', *IEEE Commun. Mag.*, 2014, **52**, pp. 129–135

[16] Akan, O.B., Ramezani, H., Khan, T., *et al.*: 'Fundamentals of molecular information and communication science', *Proc. IEEE*, 2016, **99**, pp. 1–13

[17] Colovic, M.B., Krstic, D.Z., Lazarevic-Pasti, T.D., *et al.*: 'Acetylcholinesterase inhibitors: pharmacology and toxicology', *Curr. Neuropharmacol.*, 2013, **11**, pp. 315–335

[18] Zhang, Y.G., Yang, Z., Yang, Y.L.A., *et al.*: 'Pharmacological and toxicological target organelles and safe use of single-walled carbon nanotubes as drug carriers in treating Alzheimer disease', *Nanomedicine*, 2010, **6**, (3), pp. 427–441

[19] Wang, J.T.-W., Al-Jamal, K.T.: 'Functionalized carbon nanotubes: revolution in brain delivery', *Nanomedicine*, 2015, **10**, (17), pp. 2639–2642

[20] Abbott, N.J.: 'Blood–brain barrier structure and function and the challenges for CNS drug delivery', *J. Inherit. Metab. Dis.*, 2013, **36**, (3), pp. 437–449

[21] Shityakov, S., Salvador, E., Pastorin, G., *et al.*: 'Blood-brain barrier transport studies, aggregation, and molecular dynamics simulation of multiwalled carbon nanotube functionalized with fluorescein isothiocyanate', *Int. J. Nanomed.*, 2015, **10**, pp. 1703–1713

[22] Kafa, H., Wang, J.T.-W., Rubio, N., *et al.*: 'The interaction of carbon nanotubes with an in vitro blood–brain barrier model and mouse brain in vivo', *Biomaterials*, 2015, **53**, pp. 437–452

[23] John, A., Subramanian, A.P., Vellayappan, M.V., *et al.*: 'Carbon nanotubes and graphene as emerging candidates in neuroregeneration and neurodrug delivery', *Int. J. Nanomed.*, 2015, **10**, pp. 4267–4277, article A312

[24] Tiwari, J.N., Vij, V., Kemp, K.C., *et al.*: 'Engineered carbon-nanomaterial-based electrochemical sensors for biomolecules', *ACS Nano*, 2016, **10**, (1), pp. 46–80

[25] Suzuki, I., Fukuda, M., Shirakawa, K., *et al.*: 'Carbon nanotube multi-electrode array chips for noninvasive real-time measurement of dopamine, action potentials, and postsynaptic potentials', *Biosens. Bioelectron.*, 2013, **49**, pp. 270–275

[26] Lovat, V., Pantarotto, D., Lagostena, L., *et al.*: 'Carbon nanotube substrates boost neuronal electrical signalling', *Nano Lett.*, 2005, **5**, pp. 1107–1110

[27] Cellot, G., Cilia, E., Cipollone, S., *et al.*: 'Carbon nanotubes might improve neuronal performance by favouring electrical shortcuts', *Nat. Nanotechnol.*, 2009, **4**, pp. 126–133

[28] Acker, C.D., Antic, S.D.: 'Quantitative assessment of the distributions of membrane conductances involved in action potential backpropagation along basal dendrites', *J. Neurophysiol.*, 2009, **101**, (3), pp. 1524–1541

[29] Brunner, J., Szabadics, J.: 'Analogue modulation of back-propagating action potentials enables dendritic hybrid signalling', *Nat. Commun.*, 2016, **7**, pp. 1–13

[30] Suzuki, J., Budiman, H., Carr, T.A., *et al.*: 'Simulation framework for neuron-based molecular communication', *Procedia Comput. Sci.*, 2013, **24**, pp. 103–113

[31] Balasubramaniam, S., Boyle, N.T., Della-Chiesa, A., *et al.*: 'Development of artificial neuronal networks for molecular communication', *Nano Commun. Netw.*, 2011, **2**, (2-3), pp. 150–160

[32] Nakano, T., Okaie, Y., Vasilakos, A.V.: 'Transmission rate control for molecular communication among biological nanomachines', *IEEE J. Sel. Area Commun.*, Sup. Part 2, 2013, **31**, (12), pp. 835–846

[33] Hormuzdi, S.G.: 'Electrical synapses: a dynamic signaling system that shapes the activity of neuronal networks', *Biochim. Biophys. Acta – Biomembranes*, 2004, **1662**, (1-2), pp. 113–137

[34] Galluccio, L., Palazzo, S., Enrico Santagati, G.: 'Characterization of molecular communications amongimplantable biomedical neuro-inspired nanodevices', *Nano Commun. Netw. J.*, 2013, **4**, pp. 53–64

[35] Noback, C.R., Strominger, N.L., Demarest, R.J., *et al.*: '*The human nervous system structure and function*' (Humans Press Inc., 2005)

[36] Francis, P.T.: 'The interplay of neurotransmitters in Alzheimer's disease', *CNS Spectr.*, 2005, **10**, pp. 6–9

[37] Waymire, J.C.: 'An electronic textbook for the neuroscience', *Neuroscience* (The University of Texas Medical School at Houston, Houston, USA, 1997)

[38] Abd El-atty, S.M., Gharsseldien, Z.M.: 'Influence of inter-nanoparticle interaction on nanonetworks-based molecular communications', *Int. J. Light Electron Opt.*, 2016, **127**, (5), pp. 2959–2968

[39] Abd El-atty, S.M., El-Taweel, A., El-Rabaie, S.: 'Transmission of nanoscale information-based neural communication-aware ligand–receptor interactions', *Neural Comput. Appl.*, accessed 10 March 2017, DOI: 10.1007/s00521-017-2936-5, pp. 1–14

[40] Pierobon, M., Akyildiz, I.F.: 'Fundamentals of diffusion-based molecular communication in nanonetworks', *Found. Trends Netw.*, 2014, **8**, (1-2), pp. 1–147

[41] Sidell, F.R.: '*Medical aspects of chemical and biological warfare*' (Borden Institute, Walter Reed Army Medical Center, New York, NY, 1997), pp. 131–139

[42] Smart, J.L., Andrew McCammon, J.: 'Analysis of synaptic transmission in the neuromuscular junction using', *Biophys. J.*, 1998, **75**, pp. 1679–1688

[43] Keener, J., Sneyd, J.: '*Mathematical physiology I: cellular physiology*' (Springer, Netherlands, 2008)

[44] Guney, A., Atakan, B., Akan, O.B.: 'Mobile *ad hoc* nanonetworks with collision-based molecular communication', *IEEE Trans. Mob. Comput.*, 2012, **11**, (3), pp. 353–366

[45] Bianco, A., Kostarelos, K., Partidos, C.D., *et al.*: 'Biomedical applications of functionalised carbon nanotubes', *Chem. Commun.*, 2005, **5**, pp. 571–577

[46] Webster, T.J., Waid, M.C., McKenzie, J.L., *et al.*: 'Nano-biotechnology: carbon nanofibres as improved neural and orthopaedic implants', *IOP Nanobiotechnol.*, 2003, **15**, (1), pp. 48–54

[47] Vo-Dinh, T.: '*Biomedical photonics handbook*' (CRC Press, USA, 2003), 1872pp

[48] Wang, Q.: 'Atomic transportation via carbon nanotubes', *Nano Lett.*, 2008, **9**, pp. 245–249

[49] Pantarotto, D., Briand, J.P., Prato, M., *et al.*: 'Translocation of bioactive peptides across cell membranes by carbon nanotubes', *Chem. Commun.*, 2004, **1**, pp. 16–17

[50] Ansón-Casaos, A., Grasa, L., Pereboom, D., *et al.*: 'In-vitro toxicity of carbon nanotube/polylysine colloids to colon cancer cells', *IET Nanobiotechnol.*, 2016, **10**, (6), pp. 374–381

[51] Kim, K., Chen, C.-L., Truong, Q., *et al.*: 'A carbon nanotube synapse with dynamic logic and learning', *Adv. Mater.*, 2013, **25**, pp. 1693–1698

[52] Engelman, H.S., MacDermott, A.B.: 'Presynaptic ionotropic receptors and control of transmitter release', *Nat. Rev. Neurosci.*, 2004, **5**, pp. 135–145

[53] Credi, A., Balzani, V., Langford, S.J., *et al.*: 'Logic operations at the molecular level. An XOR gate based on a molecular machine', *J. Am. Chem. Soc.*, 1997, **119**, (11), pp. 2679–2681

[54] Pearson, J.: 'Computation of hypergeometric functions', PhD thesis, University of Oxford, 2009